Identification of Hammerstein Systems with Rate-Dependent Hysteresis Nonlinearities in a Class of Smart Material-Based Actuators

Khaled F. Aljanaideh, Mohammad Al Janaideh, Micky Rakotondrabe, and Deepa Kundur

***Abstract*— In [1], we introduced an algorithm to identify rate-independent hysteresis nonlinearities of a class of smart material-based actuators, which is modeled as a Hammerstein system, that is, a cascade of a Prandtl-Ishlinskii (PI) hysteresis nonlinearity with a linear dynamic system. In this paper, we extend the results in [1] to Hammerstein systems with rate-dependent hysteresis nonlinearities. We consider a rate-dependent PI model, which has been used to model rate-dependent hysteresis nonlinearities in smart micro-positioning actuators such as piezoceramic actuators and magnetostrictive actuators. The rate-dependent hysteresis nonlinearity, the linear dynamic system, and the intermediate signal between them are assumed to be unknown. Least squares is used with a finite impulse response (FIR) model structure to identify the linear part of the Hammerstein system. Then, the output of the Hammerstein system is used along with the identified model of the linear plant to reconstruct the unknown intermediate signal. A nonparametric model of the rate-dependent hysteresis loop is obtained by plotting the reconstructed intermediate signal versus the input signal.**

I. Introduction

Smart material-based actuators such as piezomicropositioning actuators and magnetostrictive actuators have been used in different motion control applications because of their high resolution input displacement (sub-nanometers) and fast time-constant (sub-milliseconds). These smart actuators have been used in motion control applications to deliver fast output displacement in the micro/nano level in response to the applied inputs (voltage or current inputs) [2]–[4]. However, smart positioning actuators suffer from hysteresis nonlinearities that can be rate-independent or rate-dependent over different excitation frequencies in the output displacement. These nonlinearities cause high oscillations and high inaccuracies with positioning errors when these actuators operate over high frequencies [5], [6]. Therefore, it is essential to characterize the hysteresis nonlinearities over high excitation frequencies of these smart actuators in order to propose control techniques that can reduce the positioning errors.

K. Aljanaideh is with the Department of Aeronautical Engineering, Jordan University of Science and Technology, Irbid, Jordan 22110, kfaljanaideh@just.edu.jo

M. Al Janaideh is with the Department of Mechanical Engineering, Memorial University of Newfoundland, St John's, Newfoundland A1B 3X5, Canada, maljanaideh@mun.ca.

M. Rakotondrabe is with the Department of Automatic Control and Micro-Mechatronic Systems, FEMTO-ST, AS2M, Univ. Bourgogne Franche-Comté, Univ. de Franche-Comt/CNRS/ENSMM/UTBM, FEMTO-ST Institute, Besançon France, mrakoton@femto-st.fr

D. Kundur is with the Department of Electrical and Computer Engineering, University of Toronto, Toronto, Ontario M5S 2E4, Canada, dkundur@ece.utoronto.ca.

The dynamics of smart positioning actuators can be characterized by a Hammerstein system, that is, a cascade of a hysteresis nonlinearity and a linear dynamic system, see for example [5], [7]–[10]. Different models have been used to model hysteresis nonlinearties such as the Preisach model, generalized Prandtl-Ishlinskii (GPI) model, Duhem model, Bouc-Wen model, and the rate-dependent Prandtl-Ishlinskii model. The rate-dependent Prandtl-Ishlinskii model has been recently used to model rate-dependent hysteresis nonlinearities of smart material-based actuators. In [11], the rate-dependent Prandtl-Ishlinskii model has been used to model rate-dependent hysteresis nonlinearities of a piezoceramic actuator over different excitation frequencies between 10 and 200 Hz. In [12], the rate-dependent Prandtl-Ishlinskii model has been used to characterize rate-dependent hysteresis nonlinearities of a magnetostrictive actuator over different excitation frequencies between 1 and 200 Hz. In [9], the rate-dependent Prandtl-Ishlinskii model has been used to characterize rate-dependent hysteresis nonlinearities of a piezoceramic cantilever actuator over different excitation frequencies between 1 and 200 Hz. In this study, we consider a Hammerstein system with rate-dependent Prandtl-Ishlinskii model to characterize the dynamics of a class of smart material-based actuators. This Hammerstein system has been used to model different smart material-based actuators, see for example [7], [13].

Most of the Hammerstein systems identification algorithms consider Hammerstein systems with static nonlinearities [14]–[20]. In [21], identification of Hammerstein systems with hysteresis-backlash and hysteresis-relay nonlinearities was considered. However, hysteresis nonlinearities in smart positioning actuators cannot be described by hysteresis-backlash and hysteresis-relay nonlinearities. Pseudo random binary sequences were used in [6] to identify the linear dynamic part only of a piezoelectric actuator with a rate-independent hysteresis nonlinearity.

In this paper, we consider the problem of identifying Hammerstein systems with rate-dependent hysteresis nonlinearities. We assume that only the input and output of the Hammerstein system are known, where the intermediate signal of the Hammerstein system is inaccessible. The algorithm introduced in this paper consists of two stages: The first stage uses least squares with a finite impulse response (FIR) model to identify the linear part of the Hammerstein system from measurements of the input and output of the Hammerstein system. The second stage of the algorithm estimates the unknown intermediate signal using the estimated linear system and the output of the Hammerstein system. Then, a

nonparametric model of the rate-dependent hysteresis loop is obtained by plotting the reconstructed intermediate signal versus the input signal.

II. The Hammerstein system

Consider the Hammerstein system shown in Figure 1, where u is the input, $\mathcal{P} : \mathbb{R} \to \mathbb{R}$ is the rate-dependent hysteresis nonlinearity, v is the unknown intermediate signal, and y is the output of the asymptotically stable, SISO, linear, time-invariant, discrete-time system G. Note that G can represent the linear dynamics of an actuator, creep effects, and vibrations [22].

A. The Rate-Dependent Hysteresis Nonlinearity

The rate-dependent Prandtl-Ishlinskii hysteresis model has been used to model rate-dependent hysteresis nonlinearties in piezoceramic and magnetostrictive actuators [9], [12]. This rate-dependent model is constructed based on a linear combination of rate-dependent play hysteresis operators [11].

Let n be the number of rate-dependent play hysteresis operators. Then, for all $i = 1, \ldots, n$, the output of the rate-dependent play hysteresis operator $\mathcal{F}_{r_i(\bar{u}(k))}$ at time k is given by

$$\mathcal{F}_{r_i(\bar{u}(k))}[u](k) = \begin{cases} u(k) + r_i(\bar{u}(k)),\ \Delta u(k) < 0 \text{ and } \epsilon_{1,i}(k) < 0, \\ u(k) - r_i(\bar{u}(k)),\ \Delta u(k) > 0 \text{ and } \epsilon_{2,i}(k) > 0, \\ \mathcal{F}_{r_i(\bar{u}(k-1))}[u](k-1),\ \text{otherwise}, \end{cases} \tag{1}$$

where for all $i = 1, \ldots, n$, $r_i(\bar{u}(k))$ are dynamic thresholds of the rate-dependent play hysteresis operators defined by

$$r_i(\bar{u}(k)) \triangleq \xi i + \beta |\bar{u}(k)|, \tag{2}$$

$\bar{u}(k)$ is the rate of the applied input at time step k, ξ and β are positive constants obtained based on experimental data,

$$\Delta u(k) \triangleq u(k) - u(k-1), \tag{3}$$

$$\epsilon_{1,i}(k) \triangleq u(k) - r_i(\bar{u}(k)) - \mathcal{F}_{r_i(\bar{u}(k-1))}[u](k-1), \tag{4}$$

$$\epsilon_{2,i}(k) \triangleq u(k) + r_i(\bar{u}(k)) - \mathcal{F}_{r_i(\bar{u}(k-1))}[u](k-1). \tag{5}$$

The dynamic thresholds r_i, where $i = 1, \ldots, n$, have been used with the rate-dependent Prandtl-Ishlinskii model to characterize rate-dependent hysteresis nonlinearities in piezoceramic actuators [11], piezoelectric cantilever actuators [23], and magnetostrictive actuators [12].

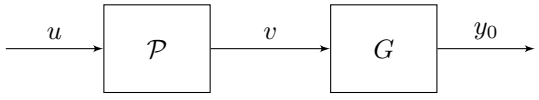

Fig. 1. Hammerstein System with a rate-dependent hysteresis model and a linear time-invariant discrete-time system G, where u is the input, $\mathcal{P}$ is the rate-dependent hysteresis nonlinearity, v is the unknown intermediate signal, and y is the output.

For all $k \geq 0$, the output v of the rate-dependent PI model is given by

$$v(k) \triangleq \sum_{i=1}^{n} p_i \mathcal{F}_{r_i(\bar{u}(k))}[u](k), \tag{6}$$

where for all $i = 1, \ldots, n$, p_i are positive weights.

Note that (1) can be written as

$$\mathcal{F}_{r_i(\bar{u}(k))}[u](k) = u(k) + q_{r_i(\bar{u}(k))}[u](k), \tag{7}$$

where

$$q_{r_i(\bar{u}(k))}[u](k) \triangleq \begin{cases} r_i(\bar{u}(k)), & \Delta u(k) < 0 \quad \text{and} \quad \epsilon_{1i}(k) < 0, \\ -r_i(\bar{u}(k)), & \Delta u(k) > 0 \quad \text{and} \quad \epsilon_{2i}(k) > 0, \\ \mathcal{F}_{r_i(\bar{u}(k-1))}[u](k-1) - u(k), & \text{otherwise}. \end{cases} \tag{8}$$

Then, using (7), (6) becomes

$$\begin{aligned} v(k) &= \sum_{i=1}^{n} p_i (u(k) + q_{r_i(\bar{u}(k))}[u](k)) \\ &= \sum_{i=1}^{n} p_i u(k) + \sum_{i=1}^{n} p_i q_{r_i(\bar{u}(k))}[u](k) \\ &= \alpha u(k) + \rho_{\bar{u}(k)}(k), \end{aligned} \tag{9}$$

where $\alpha \triangleq \sum_{i=1}^{n} p_i \in \mathbb{R}$, and

$$\rho_{\bar{u}(k)}(k) \triangleq \sum_{i=1}^{n} p_i q_{r_i(\bar{u}(k))}[u](k). \tag{10}$$

B. The Linear System

For all $j \geq 0$, let H_j denote the jth Markov (impulse response) parameter of G. Then, y_0 can be written as [24]

$$y_0(k) = \sum_{j=0}^{\infty} H_j v(k-j). \tag{11}$$

Moreover, using (9), (11) can be written as

$$\begin{aligned} y_0(k) &= \sum_{j=0}^{\infty} H_j (\alpha u(k-j) + \rho_{\bar{u}(k-j)}(k-j)) \\ &= \alpha \sum_{j=0}^{\infty} H_j u(k-j) + \sum_{j=0}^{\infty} H_j \rho_{\bar{u}(k-j)}(k-j). \end{aligned} \tag{12}$$

The identification algorithm and consistency analysis introduced here, extend the identification algorithm and consistency analysis introduced in [1] to Hammerstein systems with rate-dependent hysteresis nonlinearities.

III. Identification of the Hammerstein system

The identification problem we consider is shown in Figure 2, where u is persistently exciting of a sufficient order, w is a realization of a zero-mean, stationary, white, ergodic, Gaussian random process $\mathcal{W}$ that is uncorrelated with u, and the intermediate signal v is unknown.

A. Identification of G

We consider the FIR model G_μ of G defined by

$$G_\mu(\mathbf{q}) \triangleq \sum_{i=0}^{\mu} H_i \mathbf{q}^{-i}, \tag{13}$$

where μ is the order of G_μ. Then, using (11), the output of G can be written as

$$y_0(k) = y_{0,\mu}(k) + e_\mu(k), \tag{14}$$

where

$$y_{0,\mu}(k) \triangleq \sum_{j=0}^{\min\{\mu,k\}} H_j v(k-j), \tag{15}$$

$$\begin{aligned} e_\mu(k) &\triangleq y_0(k) - y_{0,\mu}(k) \\ &= \sum_{i=\mu+1}^{\infty} H_i v(k-i), \end{aligned} \tag{16}$$

are the output of the FIR model (13) and the modeling error in the output of the FIR model (13), respectively. Note that, taking the limit of (15) as μ tends to infinity, and using (11) yields, for all $k \geq 0$,

$$\lim_{\mu\to\infty} y_{0,\mu}(k) = \sum_{j=0}^{k} H_j v(k-j) = y_0(k). \tag{17}$$

Therefore, for all $k \geq 0$,

$$\lim_{\mu\to\infty} e_\mu(k) = y_0(k) - \lim_{\mu\to\infty} y_{0,\mu}(k) = 0. \tag{18}$$

For all $k \geq \mu$, (15) can be written as

$$y_{0,\mu}(k) = \theta_\mu \phi_v(k) + e_\mu(k), \tag{19}$$

where

$$\begin{aligned} \theta_\mu &\triangleq \begin{bmatrix} H_0 & \cdots & H_\mu \end{bmatrix}, \\ \phi_v(k) &\triangleq \begin{bmatrix} v(k) & \cdots & v(k-\mu) \end{bmatrix}^{\mathrm{T}}. \end{aligned}$$

The least squares estimate $\hat{\theta}_{\mu,\ell}$ of θ_μ is given by

$$\hat{\theta}_{\mu,\ell} = \underset{\bar{\theta}_\mu \in \mathbb{R}^{1\times\mu}}{\arg\min} \left\| \Psi_{y,\ell} - \bar{\theta}_\mu \Phi_{\mu,\ell} \right\|_{\mathrm{F}}, \tag{20}$$

where

$$\begin{aligned} \Psi_{y,\ell} &\triangleq \begin{bmatrix} y(\mu) & \cdots & y(\ell) \end{bmatrix}, \\ \Phi_{\mu,\ell} &\triangleq \begin{bmatrix} \phi_\mu(\mu) & \cdots & \phi_\mu(\ell) \end{bmatrix}, \\ \phi_\mu(k) &\triangleq \begin{bmatrix} u(k) & \cdots & u(k-\mu) \end{bmatrix}^{\mathrm{T}}, \end{aligned}$$

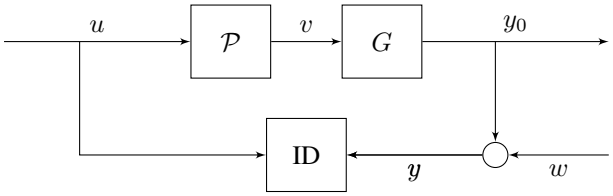

Fig. 2. Identification of the Hammerstein system, where $\mathcal{P}$ is the rate-dependent hysteresis nonlinearity, G is a linear system, u is the applied input, y is the measured output, w is the output sensor noise, and v is the unknown intermediate signal.

and ℓ is the number of samples.

It follows from (20) that the least squares estimate $\hat{\theta}_{\mu,\ell}$ of θ_μ satisfies

$$\Psi_{y,\ell}\Phi_{\mu,\ell}^{\mathrm{T}} = \hat{\theta}_{\mu,\ell}\Phi_{\mu,\ell}\Phi_{\mu,\ell}^{\mathrm{T}}. \tag{21}$$

IV. Consistency Analysis

Note from Figure 2 that for all $k \geq 0$, $y(k)$ can be written as

$$y(k) = y_0(k) + w(k). \tag{22}$$

Then, using (19), for all $k \geq \mu$, (22) can be written as

$$y(k) = \theta_\mu \phi_v(k) + e_\mu(k) + w(k). \tag{23}$$

Therefore, it follows from (23) that

$$\Psi_{y,\ell} = \theta_\mu \Phi_{v,\ell} + \Psi_{w,\ell} + \Psi_{e_\mu,\ell}, \tag{24}$$

where

$$\Phi_{v,\ell} \triangleq \begin{bmatrix} \phi_v(\mu) & \cdots & \phi_v(\ell) \end{bmatrix}, \tag{25}$$

$$\Psi_{w,\ell} \triangleq \begin{bmatrix} w(\mu) & \cdots & w(\ell) \end{bmatrix}, \tag{26}$$

$$\Psi_{e_\mu,\ell} \triangleq \begin{bmatrix} e_\mu(\mu) & \cdots & e_\mu(\ell) \end{bmatrix}. \tag{27}$$

Using (24), (21) becomes

$$(\theta_\mu \Phi_{v,\ell} + \Psi_{w,\ell} + \Psi_{e_\mu,\ell})\Phi_{\mu,\ell}^{\mathrm{T}} = \hat{\theta}_{\mu,\ell}\Phi_{\mu,\ell}\Phi_{\mu,\ell}^{\mathrm{T}}. \tag{28}$$

Using (9), note that for all $k \geq 0$,

$$\phi_v(k) = \alpha\phi_u(k) + \phi_{\rho_{\bar{u}}(k)(k)}, \tag{29}$$

where

$$\phi_{\rho_{\bar{u}}(k)(k)} \triangleq \begin{bmatrix} \rho_{\bar{u}(k)}(k) & \cdots & \rho_{\bar{u}(k-\mu)}(k-\mu) \end{bmatrix}^{\mathrm{T}}. \tag{30}$$

Therefore, using (29) we can write

$$\Phi_{v,\ell} = \alpha\Phi_{\mu,\ell} + \Phi_{\rho_{\bar{u}},\ell}, \tag{31}$$

where

$$\Phi_{\rho_{\bar{u}},\ell} \triangleq \begin{bmatrix} \phi_{\rho_{\bar{u}(\mu)}(\mu)}(\mu) & \cdots & \phi_{\rho_{\bar{u}(\ell)}(\ell)}(\ell) \end{bmatrix}. \tag{32}$$

Then, using (31), (28) can be written as

$$\begin{aligned} \alpha\theta_\mu\Phi_{\mu,\ell}\Phi_{\mu,\ell}^{\mathrm{T}} + \theta_\mu\Phi_{\rho_{\bar{u}},\ell}\Phi_{\mu,\ell}^{\mathrm{T}} + \Psi_{w,\ell}\Phi_{\mu,\ell}^{\mathrm{T}} + \Psi_{e_\mu,\ell}\Phi_{\mu,\ell}^{\mathrm{T}} \\ = \hat{\theta}_{\mu,\ell}\Phi_{\mu,\ell}\Phi_{\mu,\ell}^{\mathrm{T}}. \end{aligned} \tag{33}$$

Next, dividing (33) by ℓ and taking the limit as ℓ tends to infinity yields

$$\begin{aligned} &\alpha\theta_\mu \lim_{\ell\to\infty} \frac{1}{\ell}\Phi_{\mu,\ell}\Phi_{\mu,\ell}^{\mathrm{T}} + \theta_\mu \lim_{\ell\to\infty} \frac{1}{\ell}\Phi_{\rho_{\bar{u}},\ell}\Phi_{\mu,\ell}^{\mathrm{T}} + \lim_{\ell\to\infty} \frac{1}{\ell}\Psi_{w,\ell}\Phi_{\mu,\ell}^{\mathrm{T}} \\ &+ \lim_{\ell\to\infty} \frac{1}{\ell}\Psi_{e_\mu,\ell}\Phi_{\mu,\ell}^{\mathrm{T}} = \lim_{\ell\to\infty} \hat{\theta}_{\mu,\ell} \lim_{\ell\to\infty} \frac{1}{\ell}\Phi_{\mu,\ell}\Phi_{\mu,\ell}^{\mathrm{T}}. \end{aligned} \tag{34}$$

Since w is a realization of a white, zero-mean random process that is uncorrelated with u, then $\lim_{\ell\to\infty} \frac{1}{\ell}\Psi_{w,\ell}\Phi_{\mu,\ell}^{\mathrm{T}} = 0_{1\times\mu}$. Therefore, (34) becomes

$$\begin{aligned} &\alpha\theta_\mu \lim_{\ell\to\infty} \frac{1}{\ell}\Phi_{\mu,\ell}\Phi_{\mu,\ell}^{\mathrm{T}} + \theta_\mu \lim_{\ell\to\infty} \frac{1}{\ell}\Phi_{\rho_{\bar{u}},\ell}\Phi_{\mu,\ell}^{\mathrm{T}} \\ &+ \lim_{\ell\to\infty} \frac{1}{\ell}\Psi_{e_\mu,\ell}\Phi_{\mu,\ell}^{\mathrm{T}} = \lim_{\ell\to\infty} \hat{\theta}_{\mu,\ell} \lim_{\ell\to\infty} \frac{1}{\ell}\Phi_{\mu,\ell}\Phi_{\mu,\ell}^{\mathrm{T}}. \end{aligned} \tag{35}$$

Since u is a persistently exciting signal of a sufficient order, then $Q \triangleq \lim_{\ell\to\infty} \frac{1}{\ell}\Phi_{\mu,\ell}\Phi_{\mu,\ell}^{\mathrm{T}}$ has full rank. Therefore, multiplying (35) by Q^{-1} from the right yields

$$\alpha\theta_\mu + \theta_\mu R_{\rho_{\bar{u}}} Q^{-1} + \lim_{\ell\to\infty} \frac{1}{\ell}\Psi_{e_\mu,\ell}\Phi_{\mu,\ell}^{\mathrm{T}} Q^{-1} = \lim_{\ell\to\infty} \hat{\theta}_{\mu,\ell}, \tag{36}$$

where $R_{\rho_{\bar{u}}} \triangleq \lim_{\ell\to\infty} \frac{1}{\ell}\Phi_{\rho_{\bar{u}},\ell}\Phi_{\mu,\ell}^{\mathrm{T}}$.

Note that

$$\begin{aligned} R_{\rho_{\bar{u}}} &= \lim_{\ell\to\infty} \frac{1}{\ell}\Phi_{\rho_{\bar{u}},\ell}\Phi_{\mu,\ell}^{\mathrm{T}} \\ &= \lim_{\ell\to\infty} \frac{1}{\ell}\begin{bmatrix} \rho_{\bar{u}(\mu)}(\mu) & \cdots & \rho_{\bar{u}(\ell)}(\ell) \\ \vdots & \ddots & \vdots \\ \rho_{\bar{u}(0)}(0) & \cdots & \rho_{\bar{u}(\ell-\mu)}(\ell-\mu) \end{bmatrix}\begin{bmatrix} u(\mu) & \cdots & u(0) \\ \vdots & \cdots & \vdots \\ u(\ell) & \cdots & u(\ell-\mu) \end{bmatrix} \\ &= \lim_{\ell\to\infty} \frac{1}{\ell}\begin{bmatrix} \sum_{j=\mu}^{\ell}\rho_{\bar{u}(i)}(i)u(i) & \cdots & \sum_{j=\mu}^{\ell}\rho_{\bar{u}(i)}(i)u(i-\mu) \\ \vdots & \ddots & \vdots \\ \sum_{j=\mu}^{\ell}\rho_{\bar{u}(i-\mu)}(i-\mu)u(i) & \cdots & \sum_{j=0}^{\ell-\mu}\rho_{\bar{u}(i)}(i)u(i) \end{bmatrix}. \end{aligned} \tag{37}$$

Moreover, note that

$$\begin{aligned} Q &= \lim_{\ell\to\infty} \frac{1}{\ell}\Phi_{\mu,\ell}\Phi_{\mu,\ell}^{\mathrm{T}} \\ &= \lim_{\ell\to\infty} \frac{1}{\ell}\begin{bmatrix} u(\mu) & \cdots & u(\ell) \\ \vdots & \ddots & \vdots \\ u(0) & \cdots & u(\ell-\mu) \end{bmatrix}\begin{bmatrix} u(\mu) & \cdots & u(0) \\ \vdots & \cdots & \vdots \\ u(\ell) & \cdots & u(\ell-\mu) \end{bmatrix} \\ &= \lim_{\ell\to\infty} \frac{1}{\ell}\begin{bmatrix} \sum_{j=\mu}^{\ell}u(i)^2 & \cdots & \sum_{j=\mu}^{\ell}u(i)u(i-\mu) \\ \vdots & \ddots & \vdots \\ \sum_{j=\mu}^{\ell}u(i)u(i-\mu) & \cdots & \sum_{j=0}^{\ell-\mu}u(i)^2 \end{bmatrix}. \end{aligned} \tag{38}$$

Note from (37) and (38) that if the entries of $R_{\rho_{\bar{u}}}$ are much smaller than the entries of Q, then $R_{\rho_{\bar{u}}}Q^{-1}$ can be neglected. We choose u such that $R_{\rho_{\bar{u}}}Q^{-1}$ is small, and thus (36) becomes

$$\alpha\theta_\mu + \lim_{\ell\to\infty} \frac{1}{\ell}\Psi_{e_\mu,\ell}\Phi_{\mu,\ell}^{\mathrm{T}} Q^{-1} \approx \lim_{\ell\to\infty} \hat{\theta}_{\mu,\ell}. \tag{39}$$

Note from (18) and (27) that, as μ increases, the entries of $\Psi_{e_\mu,\ell}$ become smaller. Therefore, we choose μ to be large enough such that

$$\lim_{\ell\to\infty} \frac{1}{\ell}\Psi_{e_\mu,\ell,\mu}\Phi_{u,\ell,\mu}^{\mathrm{T}} \approx 0_{1\times(\mu+1)}. \tag{40}$$

Therefore, (39) becomes

$$\lim_{\ell\to\infty} \hat{\theta}_{\mu,\ell} \approx \alpha\theta_\mu, \tag{41}$$

which indicates that $\hat{\theta}_{\mu,\ell}$ is correct up to an unknown scalar factor.

V. Identification of the Rate-Dependent Hysteresis Nonlinearity

To identify the hysteresis nonlinearity, we first consider estimating the unknown intermediate signal v. Then, plotting the estimate $\hat{v}$ of v versus the input u will yield an estimate of the hysteresis nonlinearity [1]. Since we have a rate-dependent hysteresis nonlinearity, we consider estimating the hysteresis nonlinearity under different frequencies of the excitation signal u.

The eigensystem realization algorithm (ERA), which is based on the Ho-Kalman realization theory can be used to construct a transfer function estimate $\hat{G}$ of G from the estimated Markov parameters obtained from (20) [25], [26]. The estimate $\hat{v}$ of v can then be obtained by applying the output y as an input to the estimated transfer function $\hat{G}^{-1}$ of G^{-1}. Noncausal FIR appoximations of $\hat{G}^{-1}$ can be used if $\hat{G}^{-1}$ is noncausal or unstable [1], [24].

Suppose that $\hat{G}^{-1}$ is analytic in the open annulus $\mathbb{A}(\rho_1,\rho_2) \triangleq \{z \in \mathbb{C} : |z| > \rho_1 \text{ and } |z| < \rho_2\}$, where $\rho_1 < 1 < \rho_2$. Then, the Laurent expansion of $\hat{G}^{-1}$ in $\mathbb{A}(\rho_1,\rho_2)$ is given by

$$\hat{G}^{-1}(z) = \sum_{i=-\infty}^{\infty} \hat{h}_i z^{-i}, \tag{42}$$

where $\hat{h}_i$ is the ith coefficient of the Laurent expansion of $\hat{G}^{-1}$ in $\mathbb{A}(\rho_1,\rho_2)$. Truncating the sum in (42) yields

$$\hat{G}_{\mathrm{inv},r,d}(\mathbf{q}) \triangleq \sum_{i=-d}^{r} \hat{h}_i \mathbf{q}^{-i}, \tag{43}$$

where r and d are the orders of the causal and noncausal parts of $\hat{G}_{\mathrm{inv},r,d}$, respectively. Assuming that $\hat{G}^{-1}$ has no poles on the unit circle, then there exist finite r and d such that $\|\hat{G}^{-1} - \hat{G}_{\mathrm{inv},r,d}\|$ is negligible [24, Theorem 4.1], [27].

To obtain the estimate $\hat{v}$ of v, we use y as an input to (43), which yields, for all $k \geq r$,

$$\hat{v}(k) = \hat{G}_{\mathrm{inv},r,d}(\mathbf{q})y(k) = \sum_{i=-d}^{r} \hat{h}_i y(k-i). \tag{44}$$

Finally, a nonparametric model of the hysteresis nonlinearity is obtained by plotting the estimate $\hat{v}$ of v versus u under different frequencies of the excitation signal u.

VI. A Numerical Example

Example 6.1: In this example, we consider the transfer function

$$G(\mathbf{q}) = \frac{(\mathbf{q}+0.3)(\mathbf{q}-0.2)}{(\mathbf{q}+0.5)(\mathbf{q}-0.6)}, \tag{45}$$

and the rate-dependent play operators with the weights $p_1 = 1$, $p_2 = 0.5$, $p_3 = 0.33$, $p_4 = 0.25$, and $p_5 = 0.2$, and, for $i = 1,\ldots,5$, the dynamic threshold of

$$r_i(\bar{u}(k)) = 0.5i + 0.0001|\bar{u}(k)|, \tag{46}$$

where $\bar{u}(k) = \frac{1}{T_{\mathrm{s}}}(u(k) - u(k-1))$ and $T_{\mathrm{s}} = 0.1$ sec is the sampling time.

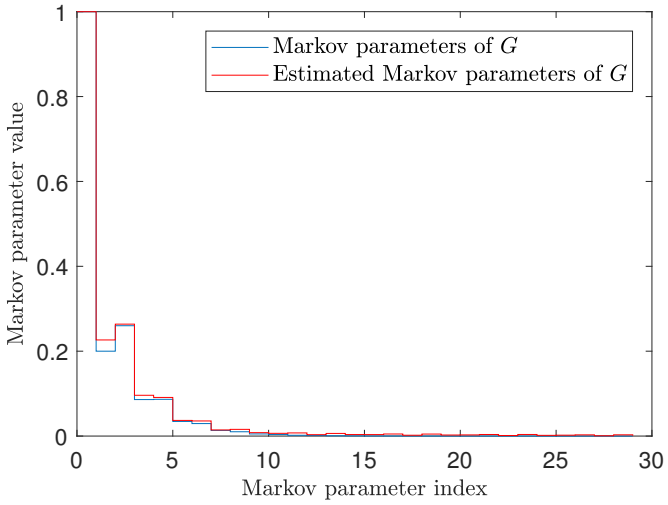

Fig. 3. Markov parameters of G and the estimated Markov parameters of G after scaling.

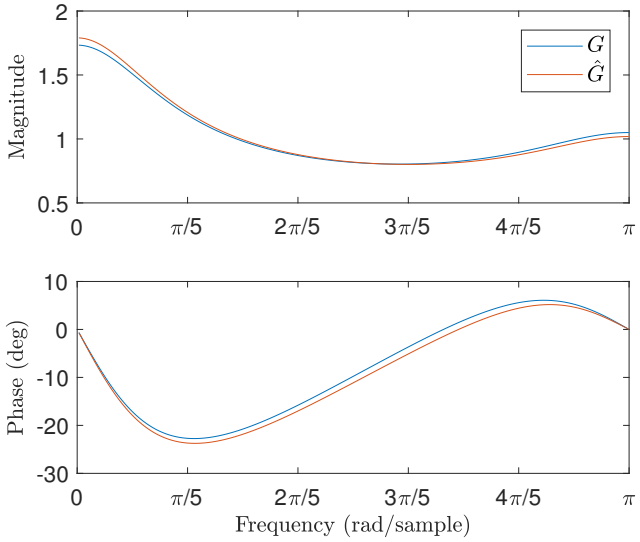

Fig. 4. Bode plot of G and the identified model $\hat{G}$.

For all $k \geq 0$, let

$$u(k) = \sum_{i=1}^{100} \sin(\omega_i T_{\mathrm{s}} k), \tag{47}$$

where for all $i = 1, \ldots, 100$, $\omega_i = i$. To identify G consider u and y with least squares and an FIR model with order $\mu = 30$. Figure 3 shows the Markov parameters of G and the estimated Markov parameters of G after scaling. Then, we construct an IIR model $\hat{G}$ of G using ERA and the estimated Markov parameters of G after scaling. Figure 4 shows the Bode plot of G and $\hat{G}$. We apply y as an input to the noncausal FIR approximation $\hat{G}_{\mathrm{inv},r,d}$ of $\hat{G}^{-1}$. Figure 5 shows the intermediate signal v and the estimate $\hat{v}$ of v, obtained by applying y as an input to the noncausal FIR approximation $\hat{G}_{\mathrm{inv},r,d}$ of $\hat{G}^{-1}$.

Next, suppose that for all $k \geq 0$, $u(k) = \sin(2\pi f T_{\mathrm{s}} k)$, where $f = 10, 50, 100,$ and 200 Hz. For each case of f, we use the output y due to the sinusoidal input u and the noncausal FIR approximation $\hat{G}_{\mathrm{inv},r,d}$ of $\hat{G}^{-1}$ to estimate the unknown intermediate signal $\hat{v}$ due to the sinusoidal input u. Finally, Figure 6 shows the true and estimated hysteresis loops obtained for $f = 10, 50, 100,$ and 200 Hz.

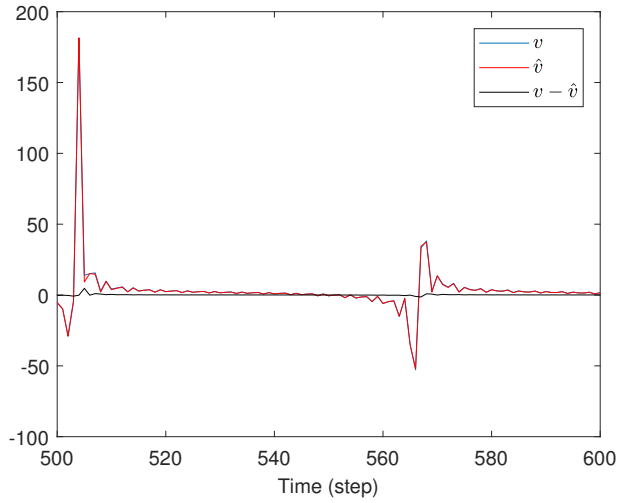

Fig. 5. Plot of the intermediate signal v and the estimate $\hat{v}$ obtained by applying y as an input to the noncausal FIR approximation $\hat{G}_{\mathrm{inv},r,d}$ of $\hat{G}^{-1}$, where u is given by (47).

VII. Conclusions

This study proposed an algorithm to identify the nonlinear dynamics of a piezomicropositioning actuator, which is modeled as a Hammerstein system, that is, a cascade of a rate-dependent PI hysteresis nonlinearity with a linear dynamic system. We showed that the estimates of the Markov parameters of the linear system obtained using least squares with an FIR model are semi-consistent, that is, correct up to an unknwon scalar factor. ERA was used to construct a transfer function estimate of the linear system from the estimated Markov parameters. An estimate of the intermediate signal was obtained by applying the output of the Hammerstein system as an input to the noncausal FIR approximation of the inverse of the estimate of the linear system. Finally, the input to the Hammerstein system and the estimate of the intermediate signal were used to obtain a nonparametric estimate of the hysteresis nonlinearity.

References

[1] K. F. Aljanaideh, M. Rakotondrabe, M. A. Janaideh, and D. Kundur, "Identification of precision motion systems with Prandtl-Ishlinskii hysteresis nonlinearities," in *American Control Conference*, Milwaukee, WI, 2018, pp. 5225–5230.

[2] S. Liang, M. Boudaoud, B. Cagneau, and S. Regnier, "Velocity characterization and control strategies for nano-robotic systems based on piezoelectric stick-slip actuators," in *International Conference of Robotic and Automation*, Singapore, Singapore, 2017, pp. 6606–6611.

[3] J. Cailliez, M. Boudaoud, S. Liang, and S. Regnier, "A multi-model design for robust hybrid control of non-linear piezoelectric actuators at the micro/nano scales," in *American Control Conference*, Milwaukee, WI, 2018, pp. 5131–5137.

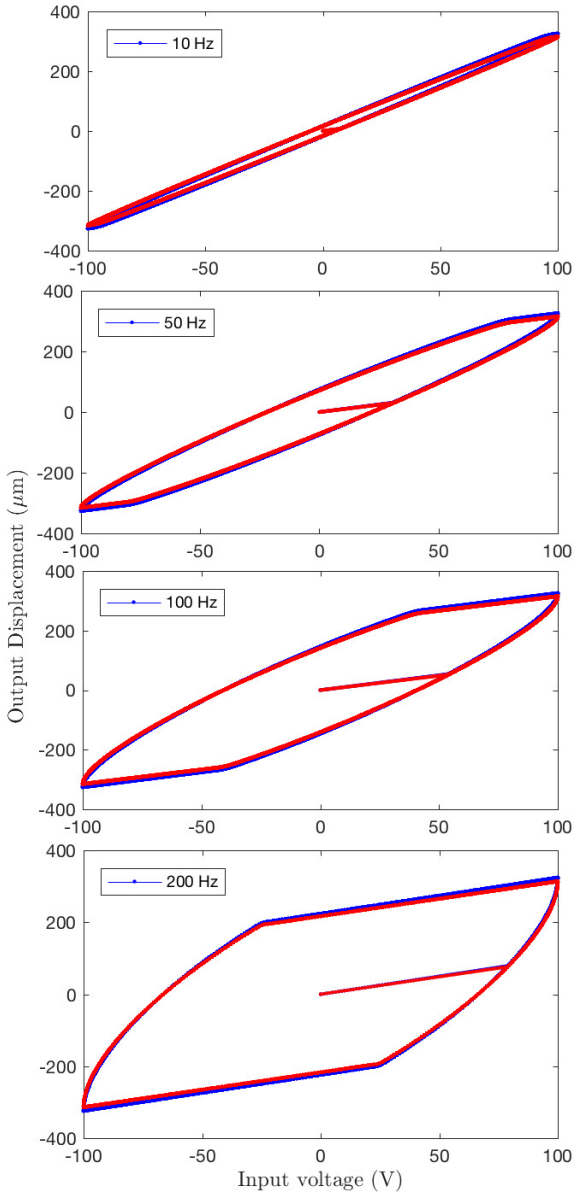

Fig. 6. True hysteresis loop (blue) and estimated hysteresis loop (red) for the case of $f = 10$ Hz, $f = 50$ Hz, $f = 100$ Hz, and $f = 200$ Hz. Note that the presented algorithm can estimate rate-dependent hysteresis loops at different frequencies.

[4] R. Subramanian, M. Heertjes, and T. Hoog, "A model-based inferential feedforward approach to deal with hysteresis in a motion system," in *American Control Conference*, Milwaukee, WI, 2018, pp. 2934–2939.

[5] L. Fang, J. Wang, and X. Tan, "An incremental harmonic balance-based approach for harmonic analysis of closed-loop systems with Prandtl-Ishlinskii operator," *Automatica*, pp. 48–56, 2018.

[6] M. Butcher, A. Giustiniani, and A. Masi, "On the identification of Hammerstein systems in the presence of an input hysteretic nonlinearity with nonlocal memory: Piezoelectric actuators – an experimental case study," *Physica B*, vol. 486, pp. 101–105, 2016.

[7] X. Tan and J. Baras, "Modeling and control of hysteresis in magnetostrictive actuators," *Automatica*, vol. 40, pp. 1469–1480, 2004.

[8] M. Edardar, X. Tan, and H. Khalil, "Design and analysis of sliding mode controller under approximate hysteresis compensation," *IEEE Transactions on Control Systems Technology*, pp. 48–56, 2015.

[9] M. Al Janaideh, M. Rakotondrabe, I. Al-Darabsah, and O. Aljanaideh, "Internal model-based feedback control design for inversion-free feedforward rate-dependent hysteresis compensation of piezoelectric cantilever actuator," *Control Engineering Practice*, vol. 72, pp. 29–41, 2018.

[10] A. Cavallo, D. Davino, G. D. Maria, C. Natale, S. Pirozzi, and C. Visone, "Hysteresis compensation of smart actuators under variable stress conditions," *Physica B: Condensed Matter*, vol. 403, pp. 261–265, 2008.

[11] M. Al Janaideh and P. Krejci, "Inverse rate-dependent Prandtl–Ishlinskii model for feedforward compensation of hysteresis in a piezomicropositioning actuator," *IEEE/ASME Transactions on Mechatronics*, pp. 1489–1507, 2013.

[12] M. Al Janaideh and O. Aljanaideh, "Further results on open-loop compensation of rate-dependent hysteresis in a magnetostrictive actuator with the prandtl-ishlinskii model," *Mechanical Systems and Signal Processing*, pp. 835–850, 2013.

[13] D. Davino, C. Natale, S. Pirozzi, and C. Visone, "Phenomenological dynamic model of a magnetostrictive actuator," *Physica B: Condensed Matter*, vol. 343, pp. 112–116, 2004.

[14] J. Schoukens, J. Nemeth, P. Crama, Y. Rolain, and R. Pintelon, "Fast approximate identification of nonlinear systems." *Automatica*, vol. 39, pp. 1267–1274, 2003.

[15] T. H. Van Pelt and D. S. Bernstein, "Non-linear system identification using hammerstein and non-linear feedback models with piecewise linear static maps," *International Journal of Control*, vol. 74, no. 18, pp. 1807–1823, 2001.

[16] B. Ninness and S. Gibson, "Quantifying the accuracy of Hammerstein model estimation," *Automatica*, vol. 38, pp. 2037–2051, 2002.

[17] E.-W. Bai, "Identification of linear systems with hard input nonlinearities of known structure," *Automatica*, vol. 38, no. 5, pp. 853–860, 2002.

[18] F. Ding, X. P. Liu, and G. Liu, "Identification methods for Hammerstein nonlinear systems," *Digital Signal Processing*, vol. 21, no. 2, pp. 215–238, 2011.

[19] K. F. Aljanaideh and D. S. Bernstein, "Nonparametric identification of Hammerstein systems using orthogonal basis functions as ersatz nonlinearities," in *ASME Dynamic Systems and Control Conference*, Palo Alto, CA, 2013, p. V003T35A004.

[20] B. J. Coffer, K. Aljanaideh, and D. S. Bernstein, "Identification of Hammerstein systems using input amplitude multiplexing," in *American Control Conference*, Washington, DC, 2013, pp. 3930–3935.

[21] F. Giri, Y. Rochdi, F. Chaoui, and A. Brouri, "Identification of Hammerstein systems in presence of hysteresis-backlash and hysteresis-relay nonlinearities," *Automatica*, vol. 44, no. 3, pp. 767–775, 2008.

[22] K. Leang and S. Devasia, "Feedback-linearized inverse feedforward for creep, hysteresis, and vibration compensation in AFM piezoactuators," *IEEE Transactions on Control Systems Technology*, vol. 15, pp. 927–935, 2007.

[23] O. Aljanaideh, M. Al Janaideh, and M. Rakotondrabe, "Enhancement of micro-positioning accuracy of a piezoelectric positioner by suppressing the rate-dependant hysteresis nonlinearities," in *Proceediongs of IEEE/ASME International Conference on Advanced Intelligent Mechatronics*, Besançon, France, 2014, pp. 1683–1688.

[24] K. F. Aljanaideh and D. S. Bernstein, "Closed-loop identification of unstable systems using noncausal FIR models," *International Journal of Control*, vol. 90, no. 2, pp. 168–185, 2017.

[25] B. Ho and R. Kalman, "Efficient construction of linear state variable models from input/output functions," *Regelungstechnik*, vol. 14, pp. 545–548, 1966.

[26] J.-N. Juang, *Applied system identification*. Prentice Hall, 1994.

[27] D. S. Bernstein, K. F. Aljanaideh, and A. E. Frazho, "Laurent series and ℓ^p sequences," *American Mathematical Monthly*, vol. 123, no. 4, pp. 398–398, 2016.